One Step Electrodeposition of $NiCo_2S_4$ Nanosheets on Patterned Platinum Electrodes for Non-Enzymatic Glucose Sensing

Padmanathan Karthick Kannan[a], Chunxiao Hu[b], Hywel Morgan*[b] and Chandra Sekhar Rout*[a]

Abstract: We describe the preparation of $NiCo_2S_4$ (NCS) nanosheets on photolithographically patterned platinum electrodes by electrodeposition. The as-prepared nanosheets were systematically characterized by field emission scanning electron microscope (FESEM), energy dispersive X-ray (EDX) and X-ray photoelectron spectroscopy (XPS) techniques. The NCS modified Pt electrode was used as a non-enzymatic glucose sensor. The sensor response exhibited two linear regions in glucose concentration, with a limit of detection of 1.2 µM. The sensors showed that the as-prepared NCS nanosheets have excellent electrocatalytic activity towards glucose with long stability, good reproducibility and excellent anti-interference property, thus demonstrating that this material holds promise for the development of a practical glucose sensor.

Introduction

Blood glucose measurements are important and necessary to manage diabetes. Most electrochemical commercial glucose sensors use enzymes that are immobilized on the electrode surface. However, enzyme based glucose sensors require particular operation conditions. In addition enzyme based biosensors have poor thermal and chemical stability, as the enzyme is highly sensitive to atmospheric condition[1]. In order to avoid these problems, recently non-enzymatic glucose sensors are being developed[2,3]. So far, various nanostructured materials like metal nanoparticles[4,5], metal oxides[6], conducting polymers[7] and their hybrid materials[8,9] have been explored as non-enzymatic glucose sensors. Carbon nanomaterials like carbon nanotubes[10], graphene and their hybrid materials[11–13]have also been widely explored as sensor active material. Recently, transition metal dichalcogenides (TMDs) are emerging as an interesting material with widespread interest because of its exceptional electrochemical properties[14]. Traditional metal oxides (TMOs)[15–17]and transition metal hydroxides (TMHs)[18,19]have been extensively investigated for the development of non-enzymatic glucose sensors. Compared to TMOs and TMHs, TMDs shows high electrical conductivity, which can increase the kinetics of electron transport, essential for an electrochemical reaction. However, there are few reports on the use of TMDs such as MoS_2, WS_2, SnS_2 and CuS in electrochemical sensor applications[20–23]

[a] Dr. P. Karthick Kannan, Dr. Chandra Sekhar Rout
School of Basic Sciences
Indian Institute of Technology Bhubaneswar
Odisha, India
E-mail: csrout@iitbbs.ac.in, pkk.matsci@gmail.com
[b] Prof. Hywel Morgan, Dr. Chunxiao Hu
Center for Hybrid Biodevices Laboratory
School of Electronics and Computer Science
University of Southampton
Southampton SO17 1BJ, United Kingdom
E-mail: hm@ecs.soton.ac.uk

Binary TMDs have attracted extensive attention because of their high electrical conductivity and electrochemical activity compared to mono TMDs. In addition, binary TMDs show enriched redox chemistry. Some binary TMDs, including $NiMoS_4$, $CoMoS_4$, $NiCo_2S_4$, $MnCo_2S_4$, $ZnCo_2S_4$ have been recently explored for supercapacitor, solar cell and photo-catalysis application[24–26]. Although binary TMDs have already been demonstrated for the abovementioned applications, there is no report on their electrochemical sensing properties. Thus, the present study explores the non-enzymatic glucose sensing properties of $NiCO_2S_4$ (NCS) nanosheets. NCS nanosheets were directly electrodeposited onto a photolithography patterned platinum electrode and the glucose sensing properties studied using cyclic voltammetry and chronoamperometric techniques.

Results and Discussion

Fig. S2 in ESI shows the photograph of the platinum electrode. Low and high magnification FESEM images of NCS nanosheets deposited on ITO are shown in Fig. 1a and b. The images show highly interconnected dense nanosheets of NCS with uniform distribution. The EDAX analysis data is shown in Fig. 1c. The data shows that the as-prepared film contains Ni, Co and S respectively. The atomic weight ratio of Ni, Co and S was estimated from the EDAX data and found to be ~ 1:2:4 suggesting the formation of $NiCo_2S_4$. Elemental mapping images of the as-deposited NCS nanosheets are shown in Fig. S3 (ESI). The images show the presence of K edge signals of Ni, Co and S respectively. All images show even distribution of Ni, Co and S which further substantiates the uniform deposition of $NiCo_2S_4$ on ITO. Fig. S4 (ESI) shows an XRD pattern of bare and NCS coated ITO. We observed similar XRD patterns with no obvious difference for bare ITO and NCS coated ITO. This could be due to the very low thickness of the NCS film which was not detectable by XRD. Therefore, in order to confirm the surface elemental composition and chemical states of Ni, Co and S, XPS analysis was carried out. Fig. 2A-C shows XPS spectra for Ni 2p, Co 2p, S 2p levels and all the peaks are found to concur with those reported for $NiCo_2S_4$[27–29]. In Ni 2p plot (Fig. 2A), the peaks at 855.2 eV and 873.3 eV correspond to Ni 2p 3/2 and Ni 2p1/2 states, indicating the presence of both Ni^{2+} and Ni^{3+} species. The results compare with those reported for the Ni^{2+} species present in the octahedral sites of NiO[30]. Similarly in Fig. 2b, the two peaks at 780.1 eV and 796 eV denotes Co 2p3/2 and Co 2p1/2 states, confirming the existence of species viz. Co^{3+} and Co^{2+}. The oxidation state of cobalt can be easily determined from the difference in the energy gap value of the main peaks and satellite peaks. For Co^{2+}, the binding energy should be approximately 6 eV compared with 9 to 10 eV for Co^{3+}[31]. In the present study, the energy gap is 6 eV confirming the presence of Co^{3+} species. Further, the presence of sulphur is confirmed from Fig. 2C, in which the peaks at 163.2 and 161.8 eV correspond to S 2p1/2 and S 2p3/2 states. The peak at 163.2 eV can be ascribed to sulphuion present on the surface, while the peak at 161.8 eV is a typical characteristic peak of S^{2-} ions in the ternary metal sulphides[32].

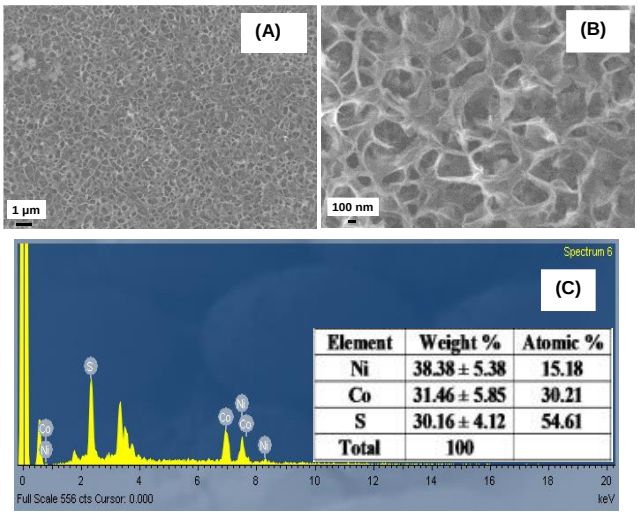

Figure 1. (A) Photograph of photolithography patterned Pt electrode used for the deposition of NCS nanosheets. (B and C) FESEM images and (D) EDAX pattern of as-prepared NCS nsnosheets.

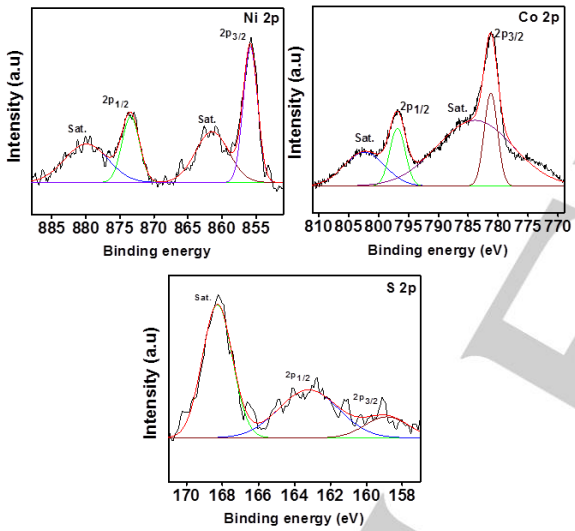

Figure 2. XPS spectra of NCS nanosheets: (A) Ni 2p (B) Co 2p (C) S 2p

In order the analyse the interfacial property of NCS/Pt, electrochemical impedance spectroscopy (EIS) was performed in 0.5 mM $K_4[Fe(CN)_6]$ solution containing 0.1 M KCl. Fig. 3 shows the Nyquist plots of bare and NCS/Pt. Bare Pt shows an inclined straight line while NCS modified Pt exhibits a depressed straight line. The charge transfer resistance (R_{ct}) value of both the bare and NCS/Pt was calculated by fitting the experimental data with the standard electrical circuit, shown inset in Fig. 3A. The equivalent circuit consists of a solution resistance (R_s) with a double layer capacitance (C), charge transfer resistance (R_{ct}) and Warburg impedance (W). R_{ct} is the charge transfer property of the redox probe and for NCS/Pt this is 18 Ohm, smaller than bare Pt (45 Ohm). The decrease in R_{ct} value is due to the high electrical conductivity of NCS which may help to increase the interfacial electron transfer thus leading to a high electrocatalytic activity.

Fig. 3B shows CV data for bare and NCS/Pt measured in 0.1 M NaOH at a scan rate of 50 mV s-1. The data shows that bare Pt does not have redox peak in the potential range between 0.1 and 0.7 V, while NCS/Pt shows a pair of well-defined oxidation and reduction peaks implying that NCS possess good electrocatalytic properties. The presence of redox peaks can be attributed to the reversible reaction of $NiCo_2S_4$ in an alkaline medium, expressed as[33]

$$NiCo_2S_4 + 2OH^- + H_2O \leftrightarrow NiSOH + 2CoSOH + e^- \quad (1)$$

$$CoSOH + OH^- \leftrightarrow CoSO + H_2O + e^- \quad (2)$$

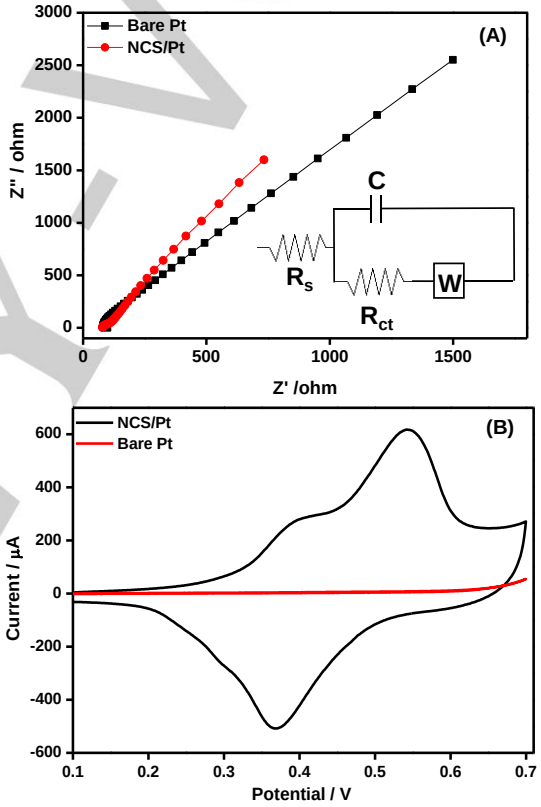

Figure 3. (A) Nyquist plot of Bare Pt and NCS/ Pt measured in 0.5mM $K_4[Fe(CN)_6]$ solution containing 0.1 M KCl. Frequency range:1 Hz – 50 KHz; DC Potential: 0.2 V; perturbation amplitude:1 mV. Inset shows fitted electrical circuit. (B) CV data of Bare and NCS modified Pt in 0.1 M NaOH. Scan rate – 50 mV s^{-1}

The electrocatalytic property of NCS/Pt towards the oxidation of glucose was ascertained from CV measurements. Fig. 4A shows CV data for NCS/Pt measured in 0.1 M NaOH containing different concentrations of glucose ranging from 0 to 5 mM. In the absence of glucose, two peaks corresponding to the reversible redox reactions of Ni^{2+}/Ni^{3+} and Co^{2+}/Co^{3+} are clearly seen. Upon addition of 0.5 mM of glucose, the oxidation peak current increases. This the peak current increases with increasing glucose indicating that NCS/Pt possesses good

electrocatalytic property towards the oxidation of glucose. The oxidation mechanism of NCS nanosheets towards glucose is described as follows: The Ni(II) species and Co (III) species present on the NCS nanosheets are converted to Ni (III) and Co (IV) due to an oxidation reaction, and in the present of glucose these oxidized species rapidly oxidizes glucose to gluconolactone, as[34]

Ni (III) +Glucose → Ni (II)+gluconolactone (3)

Co(IV)+Glucose →Co (III)+gluconolactone (4)

A plot of oxidation peak current against glucose concentration shows two linear ranges between 0.5 to 2.5 mM and 3mM to 5 mM. The plot is shown inset in Fig. 4A. Fig. 4B shows the effect of scan rate on glucose oxidation for 0.1M NaOH with 1 mM glucose, at different scan rates. Both the oxidation and reduction peak current increases with increasing scan rate (in the range 10 – 300 mV s^{-1}). The data was used to create a plot of anodic and cathodic peak current against square root of the scan rate. This shows linear dependence on scan rate, suggesting that the electrochemical process is diffusion controlled.

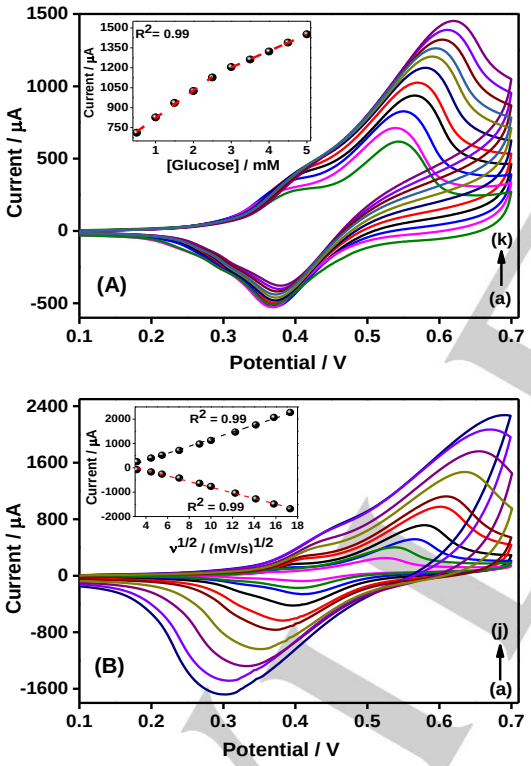

Figure 4. (A) CV data of NCS/Pt in 0.1M NaOH measured with different concentrations of glucose: a) 0 mM, b) 0.5 mM, c) 1 mM, d) 1.5 mM, e) 2 mM, f) 2.5 mM, g) 3 mM, h) 3.5 mM, i) 4 mM, j) 4.5 mM, k) 5 mM. Inset: a plot of oxidation peak current against glucose concentration. (B) CV data of NCS/Pt in 0.1M NaOH containing 1mM glucose at different scan-rates in mVs^{-1} a) 10, b) 20, c) 30, d) 50, e) 80 f) 100 g) 150 h) 200 i) 250 j) 300. Inset: plots of glucose oxidation and reduction peak current against the square root of the scan-rate.

Fig. 5A shows the amperometric response of NCS/Pt to the successive addition of different concentrations of glucose at an applied potential of 0.5 V. The NCS/Pt electrode shows rapid current changes with increasing in glucose concentration. The amperometric data was used to create a calibration plot, by plotting the peak current against glucose concentration, as shown in Fig. 5B. The plot shows two linear portions. In the concentration range 1 µM to 664 µM, the sensor response is linear with I (µA) = 0.36 (µM) + 28.8, with a sensitivity of 5.14 µA $µM^{-1}$ cm^{-2} (correlation coefficient =0.98). The second linear portion occurs between 864 µM and 5665µM with the corresponding linear equation of I (µA) = 0.09 (µM) + 220.The sensitivity is estimated as 1.3 µA $µM^{-1}$ cm^{-2} (with linear correlation = 0.98). The limit of detection (LOD) and limit of quantification (LOQ) for the NCS/Pt glucose sensor, calculated as in[35] are found to be 1.2 µM and 3.8 µM respectively

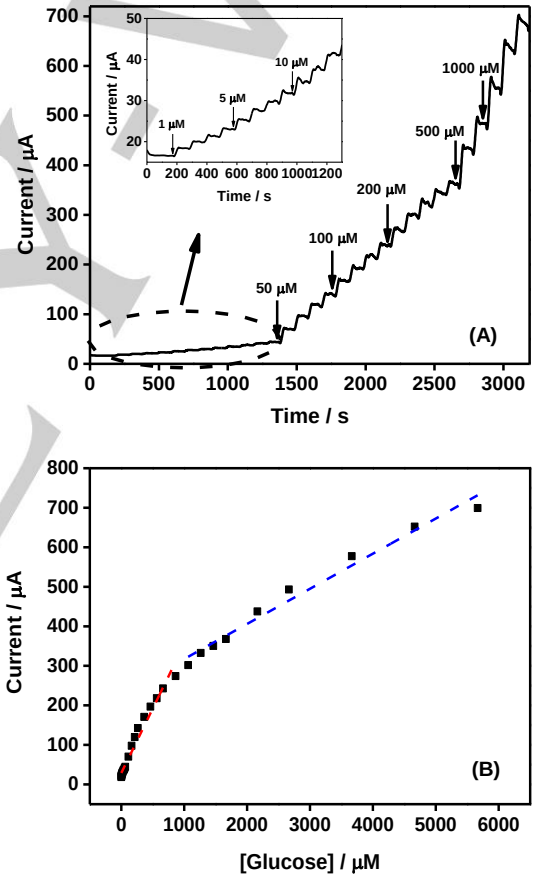

Figure 5. (A) chronoamperometric response of NCS/Pt measured in 0.1 M NaOH containing different concentrations of glucose (B) Calibration plot of the glucose sensor

The effect of potential interfering molecules on the electrochemical oxidation of glucose was studied by performing chronoamperometric measurements at an applied potential of 0.5 V; the data is shown in Fig. 6A. Interferants such as dopamine, ascorbic acid, uric acid and ions such as K^+, Na^+, Zn^+ were used for the investigation. The addition of interfering molecules does no increase the current in the same way as Glucose, indicating that the NCS/Pt glucose sensor has good anti-interference property. Similarly, selectivity of the glucose sensor in the presence of other sugar molecules such as dextrose (d), fructose (F), lactose (L), sucrose (S) and trehalose (T) is good, as shown by data in Fig. 6B. From the Fig., it can be seen that sensor 10 times less sensitivity to these sugars than to glucose. The percentage increase in current is higher for glucose compared to dextrose and fructose. Furthermore, addition of sugars such as lactose, sucrose and trehalose does not influence the sensor response suggesting that NCS/Pt exhibits good selectivity towards glucose molecules.

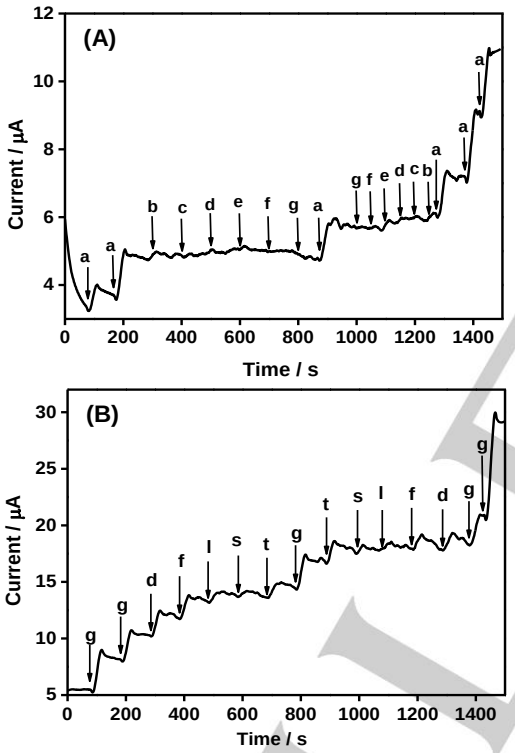

Figure 6. (A) Interference data of NCS/Pt measured in 0.1 M NaOH in the presence of (a) 1 mM of glucose and 5 mM of other interfering species *viz.* (b) dopamine (c) ascorbic acid (d) uric acid (e) K^+ (f) Na^+ (g) Zn^+. (B) Interference data of NCS/Pt measured in 0.1 M in the presence of 1mM of glucose (g) and 5 mM of dextrose (d), fructose (f), lactose (l), sucrose (s), trehalose (t). Applied potential – 0.5 V

The stability of the NCS/Pt electrode was assessed by measuring the amperometric response over a long period of time. Fig. S5 in supporting information (ESI) shows the CA response of NCA/Pt towards 0.1 mM glucose in 0.1 M NaOH at an applied potential of 0.5 V over long period of time. As can be seen, the sensor exhibits stable response over a period of 65 min indicating good stability. The electrode was stored in refrigerator for two weeks at 5 °C and then it was tested to investigate storage stability. It was found that about 94% of the initial response was maintained. The sensor also showed reproducible current with relative standard deviation of 4.2% measured over five identical electrodes.

Conclusions

Nanosheets of $NiCo_2S_4$ (NCS) have been prepared on a photolithography patterned platinum electrode using a simple electrodeposition method, The formation of $NiCo_2S_4$ along with elemental and chemical composition were confirmed by characterization techniques such as FESEM, EDAX and XPS. A non-enzymatic glucose sensor has been developed using NCS modified Pt electrode as an active material. The NCS/Pt glucose sensor showed excellent electrocatalytic activity with remarkable sensing performance, including high sensitivity, good stability and excellent anti-interference properties, making it an interesting material for the development of commercial glucose sensor.

Experimental Section

Nickel nitrate, cobalt nitrate, sodium thiosulfate and glucose were purchased from Sigma-Aldrich. Sodium hydroxide pellets were purchased from Fischer. All the chemicals were analytical grade and used as received. Millipore water was used to prepare solutions.

The area of the working electrode was 0.07 cm2 in all experiments. Thin films of $NiCo_2S_4$ nanosheets were electrodeposited onto the platinum electrode by chronoamperometry. Prior to electrodeposition, the platinum electrode was cleaned by ultrasonication in ethanol and then in water for 10 min to remove surface impurities. A working solution was prepared by mixing 0.01M nickel nitrate and 0.02 M cobalt nitrate with 0.1 M of sodium thiosulfate in 100 mL water. Electrodeposition was carried out at 70 °C. A fixed potential of 0.7V was applied for 500 s to deposit thin films of $NiCo_2S_4$ nanosheets. The crystal structure and chemical composition of the as-prepared NCS samples was assessed using XRD, FESEM, EDAX and XPS. All samples were prepared on ITO coated glass substrates in the way as for deposition on Pt electrodes. Platinum electrodes comprising reference, working and counter were fabricated on a glass substrate using photolithography. A schematic representation of the fabrication process is shown as Fig. S1 in supporting information (ESI). An in-situ Ag/AgCl reference electrode was fabricated by first electrodepositing silver onto the Pt electrode using chronoamperometry (applied potential = +0.6V, time = 300 s) by immersing the electrode in silver nitrate solution. The as-prepared silver electrode was then immersed in 0.1M KCl solution and a constant potential of +0.3 V applied for 500 s to make a Ag/AgCl electrode. FESEM measurements were performed with a MERLIN Compact with GEMINI I electron column (Zeiss Pvt. Ltd., Germany) equipped with energy dispersive X-ray spectroscopy (EDAX). X-ray photoelectron spectroscopy (XPS) was

performed using a Microtech (England instrument) Multi-Lan, ESCA-3000. All XPS experiments were carried out in ultra-high vacuum (UHV). All electrochemical measurements were performed using a Palmsens 3 potentiostat/galvanostat instrument. All experiments were performed at room temperature with 0.1 M NaOH as the supporting electrolyte. Amperometric experiments were carried out under continuous stirred condition with a potential of 0.5 V.

Acknowledgements

Dr. PKK sincerely thanks the University Grant commission, India-UK-India Education and Research Initiative (UGC-UKIERI) for the financial assistance to visit University of Southampton, United Kingdom. Dr. HM and Dr. CSR gratefully acknowledge the University Grant commission, India-UK-India Education and Research Initiative (UGC-UKIERI, Grant No. UGC-2013-14/005) for financial support

Keywords: transition metal chalcogenides • $NiCo_2S_4$ • non-enzymatic • glucose sensor • nanosheets

[1] G. Wang, X. He, L. Wang, A. Gu, Y. Huang, B. Fang, B. Geng, X. Zhang, *Microchim. Acta* **2013**, *180*, 161.

[2] K. E. Toghill, R. G. Compton, *Int J Electrochem Sci* **2010**, *5*, 1246.

[3] K. Tian, M. Prestgard, A. Tiwari, *Mater. Sci. Eng. C* **2014**, *41*, 100.

[4] Y. Fu, F. Liang, H. Tian, J. Hu, *Electrochim. Acta* **2014**, *120*, 314.

[5] B. K. Jena, C. R. Raj, *Chem. Eur. J.* **2006**, *12*, 2702.

[6] H. Cao, A. Yang, H. Li, L. Wang, S. Li, J. Kong, X. Bao, R. Yang, *Sensors Actuators, B Chem.* **2015**, *214*, 169.

[7] H. Çiftçi, U. Tamer, *React. Funct. Polym.* **2012**, *72*, 127.

[8] T. Marimuthu, S. Mohamad, Y. Alias, *Synth. Met.* **2015**, *207*, 35.

[9] K. Ghanbari, Z. Babaei, *Anal. Biochem.* **2016**.

[10] J.-S. Ye, Y. Wen, W. De Zhang, L. M. Gan, G. Q. Xu, F.-S. Sheu, *Electrochem. commun.* **2004**, *6*, 66.

[11] C. Zhang, Y. Zhang, Z. Miao, M. Ma, X. Du, J. Lin, B. Han, S. Takahashi, J. Anzai, Q. Chen, *Sensors Actuators B Chem.* **2016**, *222*, 663.

[12] M. Baghayeri, A. Amiri, S. Farhadi, *Sensors Actuators B Chem.* **2016**, *225*, 354.

[13] T. D. Thanh, J. Balamurugan, J. Y. Hwang, N. H. Kim, J. H. Lee, *Carbon N. Y.* **2016**, *98*, 90.

[14] A. Y. S. Eng, A. Ambrosi, Z. Sofer, P. Šimek, M. Pumera, *ACS Nano* **2014**, *8*, 12185.

[15] X. Cao, N. Wang, *Analyst* **2011**, *136*, 4241.

[16] S. Cherevko, C.-H. Chung, *Talanta* **2010**, *80*, 1371.

[17] K. Singh, A. Umar, A. Kumar, G. R. Chaudhary, S. Singh, S. K. Mehta, *Sci. Adv. Mater.* **2012**, *4*, 994.

[18] C.-W. Kung, Y.-H. Cheng, K.-C. Ho, *Sensors Actuators B Chem.* **2014**, *204*, 159.

[19] C. Xia, W. Ning, *Electrochem. commun.* **2010**, *12*, 1581.

[20] J. Huang, Y. He, J. Jin, Y. Li, Z. Dong, R. Li, *Electrochim. Acta* **2014**, *136*, 41.

[21] K.-J. Huang, L. Wang, Y.-J. Liu, T. Gan, Y.-M. Liu, L.-L. Wang, Y. Fan, *Electrochim. Acta* **2013**.

[22] Y. J. Yang, J. Zi, W. Li, *Electrochim. Acta* **2014**, *115*, 126.

[23] Y. Zeng, W. Li, H. Zhang, X. Wu, W. Sun, Z. Zhu, Y. Yu, *Anal. Methods* **2014**, *6*, 404.

[24] Y. M. Chen, Z. Li, X. W. (David) Lou, *Angew. Chemie* **2015**, *127*, 10667.

[25] L. Shen, J. Wang, G. Xu, H. Li, H. Dou, X. Zhang, *Adv. Energy Mater.* **2015**, *5*.

[26] X. Zheng, J. Guo, Y. Shi, F. Xiong, W.-H. Zhang, T. Ma, C. Li, *Chem. Commun.* **2013**, *49*, 9645.

[27] H. Chen, J. Jiang, L. Zhang, H. Wan, T. Qi, D. Xia, *Nanoscale* **2013**, *5*, 8879.

[28] J. Pu, T. Wang, H. Wang, Y. Tong, C. Lu, W. Kong, Z. Wang, *Chempluschem* **2014**, *79*, 577.

[29] W. Kong, C. Lu, W. Zhang, J. Pu, Z. Wang, *J. Mater. Chem. A* **2015**, *3*, 12452.

[30] J. Kim, M. Langell, *Appl. Surf. Sci.* **2000**, *165*, 70.

[31] S. Wang, Y. Hou, X. Wang, *ACS Appl. Mater. Interfaces* **2015**, *7*, 4327.

[32] T. Peng, Z. Qian, J. Wang, D. Song, J. Liu, Q. Liu, P. Wang, *J. Mater. Chem. A* **2014**, *2*, 19376.

[33] D. Cai, D. Wang, C. Wang, B. Liu, L. Wang, Y. Liu, Q. Li, T. Wang, *Electrochim. Acta* **2015**, *151*, 35.

[34] M. Wu, S. Meng, Q. Wang, W. Si, W. Huang, X. Dong, *ACS Appl. Mater. Interfaces* **2015**, *7*, 21089.

[35] P. K. Kannan, C. S. Rout, *Chem. – A Eur. J.* **2015**, *21*, 9355.

Entry for the Table of Contents (Please choose one layout)

Layout 1:

FULL PAPER

Non-enzymatic glucose sensing properties of $NiCO_2S_4$ nanosheets prepared by one step electrodeposition method is studied. The developed sensor shows high sensitivity towards glucose with good stability. In addition to that, the sensor shows excellent anti-interference property in the presence of other sugars and possible interferants species.

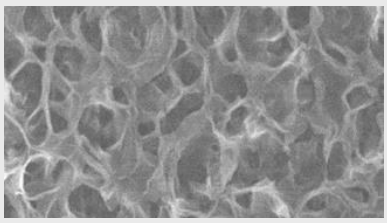

Padmanathan Karthick Kannan, Chunxiao Hu, Hywel Morgan, Chandra Sekhar Rout**

Page No. – Page No.

Title

One Step Electrodeposition of $NiCo_2S_4$ Nanosheets on Patterned Platinum Electrodes for Non-Enzymatic Glucose Sensing